Measurement and Theoretical Modeling of Protein Mobility through Membranes

A. K. Ho, J. M. Perera, D. E. Dunstan, and G. W. Stevens
Dept. of Chemical Engineering, University of Melbourne, Parkville, Victoria 3052, Australia

M. Nyström
Dept. of Chemical Technology, Lappeenranta University of Technology, FIN 53851 Lappeenranta, Finland

The electrophoretic mobilities of hemoglobin and lysozyme were measured through polycarbonate track-etched membranes of different pore sizes. Together with the zeta potential of the protein-fouled membranes, and measurements of the free-solution mobilities, protein sizes, and membrane pore sizes, the theory of Ennis et al. was tested. The presence of the membrane offered little hindrance to protein transfer when the membrane pore size was large in comparison with the protein size and the thickness of the electrical double layers. Under some solution conditions, protein agglomeration was significant and the interactions between the larger particles, and the membrane pore walls caused a more pronounced reduction in the protein mobility from its free-solution value. Good agreement with the theoretical model was found only for cases where the solution remained as a monodispersed suspension of protein monomers.

Introduction

Many processes in the biotechnology industry involve the separation and purification of biological materials from other species in solution. Electrophoresis has been recognized as a powerful technique for achieving these processes because of its high selectivity and high resolution. It relies on the different rates of migration of molecules in an applied electric field, and thus separates components of a mixture on the basis of charge and size. It is also an inherently gentle technique that, unlike traditional separation processes involving heat or shear, avoids the denaturation of delicate biological macromolecules. A further advantage is the possibility of this technique being economically competitive with existing techniques such as fractional precipitation and liquid chromatography, which require expensive media and reagents and suffer inefficiencies due to liquid channeling.

Although attractive on a microscale, current electrophoretic separation devices still face limitations in size and processing rates due to undesirable mixing and dispersion caused by natural convection as a result of Joule heating. The use of synthetic membranes in these devices has been identified as a potential technique for larger-scale operations, both as a means of separation and as a hydrodynamic barrier to control flow and mixing of solutions. The theoretical analysis of protein electrophoresis through membranes is, however, complicated by the presence of rigid membrane walls that impose perturbations on the electric field and on the surrounding flow field. Since most membranes are charged, the effect of electroosmotic flow also needs to be considered.

Recently, Ennis et al. (1996) developed a model to account for the presence of membrane pore walls in the transfer of charged spherical colloid particles with arbitrary double-layer thickness but low surface zeta potentials. The model was found to be satisfactory for the electrophoresis of bovine hemoglobin in sodium acetate buffer of ionic strength 0.075 M and pH 5.0 at 20°C, for a protein pore-size ratio of less than 0.5–0.6 where no overlapping of double layers occurred. Unfortunately, only limited experimental data were gathered, and the experiments were conducted using membranes not only of different materials but also with different pore structures and morphologies. In order to determine the limitations of the theory in predicting the mobility of proteins through membranes particularly as the size of the protein approaches the pore size, and to determine the minimum pore size usable in the electrophoresis apparatus, we aim to provide in this work a more complete analysis of the membrane–electrophoresis process.

Correspondence concerning this article should be addressed to G. W. Stevens.

Background

Fractionation of proteins using ultrafiltration or microfiltration membranes has been a subject of many studies (see, for example, Ehsani, 1996; Ehsani et al., 1997; Fane et al., 1983a,b; Ghosh and Cui, 1998; Hanemaaijer et al., 1989; Heath and Belfort, 1992; Higuchi et al., 1993; Howell et al., 1993; Lucas et al., 1998; Metsämuuronen et al., 1997; Miyama et al., 1988; Musale and Kulkarni, 1997; Nakao et al., 1988; Nyström et al., 1989, 1994, 1998; Pihlajamäki et al., 1993; Saksena and Zydney, 1994; Van Eijndhoven et al., 1995). Although the performance of such processes can be limited by fouling and electroosmotic flow, a selectivity of up to 220 has been reported (Ghosh and Cui, 1998) for the fractionation of bovine serum albumin (BSA) and lysozyme with the right choice of membrane material, by membrane pretreatment, and by utilization of electrostatic interactions. Even for proteins of similar molecular sizes, such as BSA and hemoglobin, selectivity values of more than 70 have been achieved (Van Eijndhoven et al., 1995). On the other hand, electrophoresis is a useful technique for protein separation and purification, although it is limited in scale by convective mixing. Gels and capillaries have been used that make large-scale operations impractical despite their effectiveness in suppressing mixing. Experiments have also been performed with some success under conditions of zero gravity in a space shuttle (Cogoli and Tschopp, 1982), although this appears to be a somewhat expensive solution to the problem.

As mentioned previously, the combination of electrophoresis and membrane fractionation provides an attractive alternative to large-scale protein separation. A brief review of a selection of such processes is given below.

Electrokinetic membrane separation processes

Electrodecantation is an electrokinetic separation technique that makes use of membranes to achieve stratification of colloidal components in an applied electric field (see, for example, Stamberger, 1946). The mixture to be separated is contained in a compartment formed between two membranes, behind which are located the anode and cathode, respectively. Migration of species toward the membranes occurs according to their charge, and the layer of colloids accumulated at the membrane surface will eventually move up or down depending on its density relative to that of the surrounding medium. Refinement of the technique makes use of electroosmosis to augment particle coagulation at the membrane/fluid interface to produce a more compact layer for periodic removal by reversal of electrode polarity. Examples of separation processes based on this principle include Bier's continuous-flow membrane-electrophoresis device (Bier, 1959) in which a protein-impermeable membrane is placed partway down in between two semipermeable electrode compartment membranes, and his later development that uses a porous filter as the central membrane (Hannig, 1967). This later design is said to have an improved degree of separation, as a kind of reflux is formed when a pressure difference is applied across the central membrane, resulting in bulk flow that opposes the electrophoretic migration due to the imposed potential gradient.

Another design pioneered by Bier and his coworkers is the recycling isoelectric focusing (RIEF) system for continuous electrophoresis of proteins based on differences in their isoelectric points (Bier et al., 1979). In single-pass operations, the high electric fields necessary for achieving high resolutions are limited by heat buildup and associated thermal problems. In the RIEF device, the mixture to be separated circulates between the separation compartments (a thin channel segmented by a number of microporous membranes) and external heat-transfer loops. The components migrate laterally across the membrane boundaries until they are focused into the compartment nearest their isoelectric point. The repeated intermittent electromigration and external heat transfer provides a long, effective sample residence time, which allows low field strengths to be applied—an advantage, as higher-conductivity buffers necessary for enhanced protein stability can be used. Like all isoelectric focusing systems, some of the inherent limitations include the high costs of the ampholytes and the tendency of proteins near their isoelectric points to precipitate, which results in membrane fouling and electroosmotic dispersion. Further, the carrier ampholytes must also be removed from the product after focusing. Nevertheless, this device has evolved into several commercial devices, such as the IsoPrep (Ionics, Inc., Watertown, MA) and the ATIsolator (Ampholife Technologies, Woodlands, TX) (Hunter, 1995).

Righetti et al. (1987) also constructed a RIEF apparatus, but the separation membranes were prepared with immobilized ampholytes at fixed pH values and each compartment was filled with an ampholyte buffer having a pKa intermediate between the adjacent membranes. The buffer ampholytes can be removed from the purified protein easily, as they are low molecular weight zwitterions, and the problem of removing commercial ampholytes is avoided. The recycle concept with membranes has also been extended to continuous-flow zone electrophoresis by Gobie et al. (1985) and Gobie and Ivory (1988).

A more recent development in the membrane-electrophoresis of protein mixtures is reported in the work of Liu et al. (1996a,b). This new preparative electrophoresis method, named "multichannel flow electrophoresis" (MFE), can be operated in either continuous mode or dynamic mode. It makes use of a membrane-spaced 5-compartment electrolyzer in which the central compartment and its neighboring compartments are used, respectively, for sample loading and product discharging. The electric field is applied perpendicular to the flow of the protein solution to transfer the charged components from the central compartment to their corresponding elution compartments to be washed out by carrier flow, while the neutral component is carried through the central compartment. Gel membranes used in their initial studies (Liu et al., 1996a) yielded only 13.2 mg BSA and 20.0 mg Hb per hour. Their later work (Liu et al., 1996b) made use of microfiltration membranes to take advantage of the larger pore size to give a reduced protein transmembrane resistance. This resulted in an improved yield of 56 mg BSA and 48 mg Hb per hour. The effectiveness of poly(vinyl alcohol) as a shielding polymer to reduce binding of proteins onto the membranes during the MFE process was also demonstrated.

The process of coupling membrane separation with electrophoresis is described by Hong and Lee (1986) as a means of reducing concentration polarization, the major limiting

factor in ultra- and microfiltration. Proteins and other high molecular weight materials are convected toward the upstream face of the membrane by bulk flow and leave by diffusion only, reducing the solvent flux as a result of the formation of a gel layer or a concentrated layer of increased osmotic pressure. The problem can be alleviated by applying an electric field to pull the molecules localized in the concentration polarization layer in a direction opposite to the pressure-driven convective flow. Thus by power adjustment of the electric-field strength and the applied pressure, the formation of the concentration polarization layer can be minimized while a high flow rate is maintained. The improvement in flux may be substantial, for example, Iritani et al. (1992) reported an 80% improvement at a field strength of only 4 V/cm. In addition, charged protein molecules adsorbed onto the membrane, or charged functional groups of the membrane material, establish an electroosmotic flow through the membrane pores which further increases flux (Hunter, 1995).

Other electrokinetic membrane separation methods, such as electrodialysis of electroosmotic processing (Weatherley, 1994) are more useful for the separation of ions and other low molecular-weight products, or for the recovery and purification of reagents, and are less useful for the actual separation of larger macromolecules such as proteins.

While a complete survey of available electrically driven membrane separation processes has not been included, our review highlights the fact that there have been few developments or studies concerning processes actually involving the passage of protein through the membranes. Clearly, this is an area in need of further investigation.

Effect of membrane electrochemical properties

The separation characteristics of ultrafiltration and microfiltration membranes depend on their physical properties, such as their porosity, pore-size distribution, and pore structure. The electrochemical properties of the membrane surfaces and the dispersed solutes may also have a significant influence on the nature and magnitude of the membrane-solute interactions. In fact, the fouling of membranes by dispersed materials such as proteins is known to be dependent on the relationship between the zeta potential of the membranes and the charge on the proteins. Much work has been done on characterizing the electrochemical properties of a number of polymeric and inorganic membranes using different methods, giving widely differing results (see, for example, Causserand et al., 1994; Ehasni, 1996; Kim et al., 1994a, 1996, 1997; Le Bolay and Ricard, 1995; Nabe et al., 1997; Nyström et al., 1989, 1994; Pontié et al., 1997; Szymczyk et al., 1997; Tracey and Davis, 1994). Determination of zeta potentials of clean and fouled membranes has largely been done through the membrane pores using streaming potential or electroosmotic techniques, with limited information on the zeta potential over the membrane surface.

Of interest in this work is the polycarbonate track-etched (PCTE)-type membranes that have straight cylindrical pores and a narrow pore-size distribution, although the porosity is rather low. The zeta potential of these membranes will be determined from two independent techniques that measure the streaming potential through the pores and over the membrane surface, in order to gain a better understanding of the effects of protein adsorption.

Effect of membrane pore size

The membrane pore size in relation to the size of the macromolecules in solution determines the extent of interactions between the solute and the membrane, and therefore affects the mobility. The effect of membrane pore size has been investigated by a number of workers. For example, Ohya et al. (1989) found that no transfer of egg albumin occurred through track-etched Nuclepore membranes of pore sizes less than 0.03 μm and concluded that the minimum pore size for any transfer of egg albumin to occur was 10 times its Stokes–Einstein radius. More recently, O'Connor (1994) found that the mobility of hemoglobin through a membrane of pore size 0.025 μm (equivalent to 8 times the Stokes radius) was 26% lower than that through a pore size of 0.2 μm. In the larger pores, the measured mobility was not discernibly affected by the pore size because the effective potential gradient across the membrane increases in inverse proportion to the free area for nonconducting membranes.

The dependence of mobility on membrane pore size is expected to be a function of the solution ionic strength, as the ionic strength influences the thickness of the double layer of the membrane pore wall and that of the solute, and this in turn determines whether overlapping of the double layers occurs. The effect of particle movement in the presence of a large plane surface has been obtained for two special cases: movement normal to a conducting plane (Morrison and Stuckel, 1970), and movement parallel to a nonconducting surface (Keh and Chen, 1988). Movement of a sphere near a single-plane wall and inside a long pore has also been investigated by Keh and Anderson (1985) using the method of reflections for the case of thin double layers, that is, at high ionic strengths where the overlapping effects diminish. This model is restricted to high κa values ($\kappa a > 30$), where κ is the reciprocal of the characteristic width of the double layer, and a is the particle radius.

The restriction to high κa values is valid for typical colloidal systems, but often not in protein electrophoresis, as the protein radius can be of the order of nanometers and the ionic strengths are often low. Ennis et al. (1996) realized this limitation and extended the analysis to cover low κa values, although it was restricted to low surface potentials. Details of the derivations are given in the original articles (Ennis and Anderson, 1997; Ennis et al., 1996). A brief summary of this model is presented here.

Theoretical model: The model of Ennis et al.

The theory of Ennis et al. (1996) was derived for spherical particles of radius a with a uniform zeta potential ζ_p in a uniform electric field E_∞. The governing equations (Eqs. 1 to 4) are given below.

Poisson's equation relates the electrostatic potential ψ at position r to the charge density ρ:

$$\nabla^2\psi(r) = -\frac{4\pi}{\epsilon}\rho(r), \tag{1}$$

where

$$\rho(r) = \sum_{j=1}^{N} z_j e n_j(r) \tag{2}$$

and z_j is the valence of ions of type j; $n_j(r)$ is their number density; e is the elementary charge; ϵ is the dielectric permittivity, which in SI units equals $4\pi\epsilon_0\epsilon_r$; ϵ_0 is the dielectric permittivity of free space; and ϵ_r is the dielectric constant or relative permittivity of the fluid.

Stokes' equation describes the fluid flow:

$$\eta\nabla^2 v - \nabla p = p\nabla\psi, \tag{3}$$

where v is the fluid velocity, p is the pressure, and η is the viscosity of the fluid. For incompressible fluids, the condition $\nabla v = 0$ is also satisfied.

For each ion, a force balance gives:

$$-\lambda_j(u_j - v) - z_j e\nabla\psi - kT\nabla\ln(n_j) = 0, \tag{4}$$

where u_j is the ion drift velocity, λ_j is the ion drag coefficient, k is Boltzmann's constant, and T is the absolute temperature. $\nabla(n_j u_j) = 0$ for each ion j due to ion conservation.

Far from the particle, disturbances to the electric and flow fields due to the particle vanish. At the surface of the particle or boundary, the boundary conditions are given by Eqs. 5 to 7:

$$v = v^* \tag{5}$$

$$\hat{n}(u_j - v^*) = 0 \tag{6}$$

$$\hat{n}\nabla\psi = -\frac{4\pi\sigma}{\epsilon}, \tag{7}$$

where v^* is the velocity of the interface, equal to zero for the fixed rigid boundary and $(U + \Omega \times r)$ for a particle translating with velocity U and rotating at angular velocity Ω; $\hat{n}$ is the outward normal into the fluid phase; and σ is the surface charge density, assumed to be constant on each surface separately.

It was assumed that the particle moves along the axis of the cylindrical pore of radius d with a uniform zeta potential ζ_w on the walls. The mobility of a particle in a closed system moving under the influence of the applied field was modeled by breaking the problem into two subproblems: (1) a particle moving in an electric field in an open system (no backflow), and (2) a particle moving in a closed system by Poiseuille flow, in the absence of an electric field. Then by using the ''method of reflections'' to iteratively adjust boundary conditions at the wall and at the particle surface, and by combining the two subproblems into one, the equation for particle mobility for the situation of interest is obtained.

The idea of the ''reflections'' is that the presence of the membrane will create a disturbance in both the electric and flow fields, and these will affect the average velocity of the particle. In electrophoresis, the particle creates a velocity disturbance that decays as r^{-3} from the center of the sphere. The no-slip assumption on the surface of the membrane pore wall implies that the wall must reflect this velocity to maintain zero velocity, at an amount proportional to d^{-3}. Similarly, the particle disturbs the electric potential of the solution by some amount, and this disturbance also decays as r^{-3}. Now the constant pore wall zeta potential assumption requires that the disturbance be reflected by the wall to the particle, again by an amount proportional to d^{-3}. These reflections of the velocity and electric potential by the sphere and the pore wall can be continued, and provided that there is minimal overlap of the double layers, will result in an expression for the average particle velocity in terms of a power series in λ, defined as the ratio of the particle radius to the membrane pore radius.

The average velocity of a particle undergoing electrophoresis in the system of interest is given by the following equation [Eq. 42 in the work of Ennis et al. (1996); see the original reference for an explanation of symbols, etc.]:

$$U(\lambda,\gamma) = \frac{\epsilon\zeta_p}{4\pi\eta}E_\infty e_z\left[\begin{array}{c} f(\kappa a) + \gamma\left(g(0,\kappa d)\dfrac{1+3.867\lambda-1.907\lambda^2-0.834\lambda^3}{1+1.867\lambda-0.741\lambda^2} - g(\lambda,\kappa d)\right) \\ +\lambda^3\{d_4[f(\kappa a)-L(\kappa a)]+d_5[L(\kappa a)-\gamma]\}+\lambda^5 d_6[L(\kappa a)-\gamma] \\ +\lambda^6\{d_4^2[f(\kappa a)-L(\kappa a)]+d_4 d_5[L(\kappa a)-\gamma]\} \end{array}\right] + O(\lambda^8) \tag{8}$$

Since the mobility is defined as the velocity of the particle per unit field strength (U/E_∞) the ratio of the velocity through the membrane pores, $U(\lambda,\gamma)$, to that in free solution, $U(0,\gamma)$, is equivalent to the ratio of their mobilities—the ''relative mobility'' μ_{rel}. Dividing Eq. 1 by the same equation with λ set to 0 gives

$$\mu_{\text{rel}} = \frac{1}{f(\kappa a)}\left[\begin{array}{c} f(\kappa a) + \gamma\left[g(0,\kappa d)\dfrac{1+3.867\lambda-1.907\lambda^2-0.834\lambda^3}{1+1.867\lambda-0.741\lambda^2} - g(\lambda,\kappa d)\right] \\ +\lambda^3\{d_4[f(\kappa a)-L(\kappa a)+d_5(L(\kappa a)-\gamma)]\}+\lambda^5 d_6[L(\kappa a)-\gamma] \\ +\lambda^6\{d_4^2[f(\kappa a)-L(\kappa a)]+d_4 d_5[L(\kappa a)-\gamma]\} \end{array}\right], \tag{9}$$

where

$$\lambda = \frac{a}{d} \tag{10}$$

$$\gamma = \frac{\zeta_w}{\zeta_p} \tag{11}$$

$$f(\kappa a) \approx \frac{2(\kappa a)^3 + 51(\kappa a)^2 + 242(\kappa a) + 208}{2(\kappa a)^3 + 57(\kappa a)^2 + 363(\kappa a) + 312} \tag{12}$$

$$L(\kappa a) \approx \frac{(\kappa a)^4 + 14(\kappa a)^3 + 58(\kappa a)^2 + 112(\kappa a) + 84}{(\kappa a)^4 + 14(\kappa a)^3 + 42(\kappa a)^2} \tag{13}$$

$$g(\lambda, \kappa d) = 1 - e^{-\lambda \kappa d}\left[\frac{\lambda^2 \kappa d}{3} + \frac{\lambda^2}{6} + \frac{1}{\kappa d}\left(2 + 3\lambda + \frac{15\lambda^2}{4}\right) - \frac{1}{(\kappa d)^2}\left(1 + \frac{9\lambda}{4} + \frac{15\lambda^2}{4}\right)\right], \tag{14}$$

where d_4, d_5, and d_6 have values 0.79683, -1.28987, and 1.89632, respectively.

In Eq. 9, the terms involving $f(\kappa a)$ originate from the ''squeezing'' of the electric field, which tends to enhance the particle velocity in the direction it would travel in bulk electrophoresis. The terms involving $L(\kappa a)$, which always dominate for a finite κa, account for viscous retardation, which tends to decrease the particle velocity. The terms γ account for the effect of the electric-field disturbance on the local electroosmotic flow. The thin double layer results in Keh and Anderson (1985) are recovered as $\kappa a \to \infty$, when both $f(\kappa a)$ and $L(\kappa a)$ tend to 1.

The model of Ennis et al. (1996) predicts that the mobility of proteins through membranes approaches the free solution value when the pore size is much bigger than the protein ($\lambda \to 0$). At intermediate pore sizes, the mobility through membranes may be significantly enhanced or reduced depending on the sign of the zeta potential ratio. At small pore sizes ($\lambda \to 1$), the mobility through membranes becomes significantly reduced due to double-layer overlapping effects.

Experimental Details

Materials

Polycarbonate track-etched membranes obtained from PORETICS (OSMONICS) U.S.A. were used. These membranes are protein-permeable, not electrically conducting, and wettable in aqueous solutions. The properties of the membranes used in this work are given in Table 1.

AR grade reagents, sodium acetate (NaAc), glacial acetic acid, 2-(*N*-morpholino)ethanesulfonic acid (MES, free acid and sodium salt forms), *tris*(hydroxymethyl)aminomethane (TRIS) and HCl, were used in the preparation of buffers and for pH adjustment.

Protein solutions were prepared as previously described (O'Connor et al., 1996). Both hemoglobin (Hb) and lysozyme (Lys) were obtained from the Sigma-Aldrich Chemical Company. Details of the two proteins are given in Table 2.

Table 1. Characteristics of the Membranes Used*

Membrane	Nominal Pore Size (μm)	Catalog No.	Pore Density (Pores/cm^2)	Typical Porosity (%)**	Thickness (μm)
PC0.2	0.20	19,413	3×10^8	9.42	10
PC0.2(L)†	0.20	19,414	7×10^7	2.20	10
PC0.1	0.10	19,410	4×10^8	3.14	6
PC0.08	0.08	19,407	4×10^8	2.01	6
PC0.05	0.05	19,405	6×10^8	1.18	6
PC0.03	0.03	19,403	6×10^8	0.42	6
PC0.01	0.01	19,401	6×10^8	0.05	6

Source: PORETICS (1996).
*Material: polycarbonate (PC); wetting characteristics: hydrophilic; wetting agent: polyvinylpyrrolidone (PVP); adsorption losses: low; typically 3–6%.
**Calculated from the pore density (pores/cm^2) and assuming that the pores have circular cross sections.
†''L'' signifies low pore density (nonstandard type).

Equipment and methods

Mobility Measurements. Through-pore mobility measurements were carried out in a membrane-electrophoresis cell, details of which have been previously described (O'Connor et al., 1996; Ennis et al., 1996). The measurements were carried out under conditions of zero initial concentration gradient between the two protein compartments, with a feed concentration of approximately 0.2 mg/mL in all cases. The experimental conditions are summarized in Table 3.

The effective mobility, μ, through the membrane pores is given by the equation

$$\mu = \frac{VK}{A_o i}\left(\frac{dA}{dt}\right)_{t=0}, \tag{15}$$

where V is the volume of the monitored protein chamber, K is the solution conductivity, i is the electric current, and A_o and $(dA/dt)_{t=0}$ are the initial absorbance and initial rate of change of absorbance, respectively. In all cases, the rate of protein depletion was monitored (O'Connor et al., 1996), with the electrode configuration and the sign of the mobility adjusted accordingly.

Free-solution mobilities were measured at the same conditions as for the membrane-electrophoresis experiments, using the *Coulter DELSA 440*. This combines the techniques of electrophoresis and laser Doppler velocimetry, and has the advantage of measuring mobilities without the effect of supporting media. The system consists of a sample chamber that is located in the optical bench. Light-scattering signals are sent to the computer for processing and analysis, and a remote power supply provides regulated voltages to the optical bench. Details of the apparatus are described in the *Coulter DELSA 440* manual (Coulter, 1988).

A carefully dispersed suspension of protein molecules was prepared and injected into the sample cell with a syringe via the fill tube. When no bubbles were found in the hemispherical reservoirs and the channel, the cell was placed into the sample chamber compartment of the optical bench.

Table 2. Characteristics of the Proteins Used

	Hemoglobin	Lysozyme
Catalog number (Sigma-Aldrich)	H-2500	L-6876
Lot number	46F-9305	65H-7025
Source	Bovine blood	Chicken egg white
Molar mass (g/mol)	68,000 (Walters et al., 1984)	14,300 (Sigma-Aldrich)
Equivalent spherical radius (nm)	3.1, 3.4 (Fox and Foster, 1957) 4.8** (Zhang, 1996)	1.6, 1.9* (Chae and Lenhoff, 1995)
Diffusion coefficient (cm^2/s, 20°C, at infinite dilution)	$(7.32 \pm 0.18) \times 10^{-7}$ (Walters et al., 1984) 6.9×10^{-7} (Cantor and Schimmel, 1980)	$(8.6 \text{ to } 11.2) \times 10^{-7}$ (Fox and Foster, 1957)
Shape	Roughly spherical (Merck Index, 1983)	Ellipsoidal (Chae and Lenhoff, 1995)
Isoelectric point	6.8 (Lehninger, 1982) 7.0 (Fox and Foster, 1957)	10.5–11.0 (Merck Index, 1983)
Composition/purity	Up to 75% methemoglobin, Balance primarily oxyhemoglobin	Contains less than 5% buffer salts such as NaAc and NaCl
Wavelength for max absorbance (nm)	405 (O'Connor, 1994)	280 (Zhang, 1996)
Extinction coefficient (cm^2/mg)	7.81 (O'Connor, 1994)	2.203 (Zhang, 1996)

*Ellipsoidal radius.
**Obtained experimentally by dynamic light scattering.

The usual method for measuring the true electrophoretic mobility is at the stationary layer, where the electroosmotic velocity is zero. Measurements at the stationary layer normally involve finding the location of the sample cell walls by viewing the laser beams under the built-in microscope, adjusting the beam intersection and intensity, and finally positioning the cell to the desired level using a motor optical encoder combination.

Initial trials with hemoglobin showed that, due to the small particle size, very little light scattering occurred such that it was extremely difficult to locate the cell walls [the instrument is suitable for particles whose sizes range from 0.01 to 30 μm (Coulter, 1988)]. The results contained substantial scatter as they were sensitive to the position at which the measurements were made. A different approach was therefore adopted, based on that described by Pelton et al. (1993), and involved the Komagata plot (Hunter, 1981).

First, a rough estimate of the location of the top cell wall was made by performing an A/D converter test (instead of visual observations of laser beams, due to weak light scattering) in the *DELSA* and noting where the sudden dip in light intensity occurred with respect to a small change in the vertical position of the sample cell. The dial indicator (micrometer) located on top of the optical bench was zeroed at this position, and mobility measurements were then made at positions in the cell between "20" and "80," in increments of 10 units (positions "0" and "100" correspond to the upper and lower cell walls, respectively). Although the measurements were made at all four angles (8.6°, 17.1°, 25.6°, and 34.2°) (7.5°, 15°, 22.5°, and 30° before correction for refractive index), only the peak at the smallest scattering angle was used in the analysis. The spectra of small particles at the higher angles would indicate the presence of aggregates or multimeric structures.

The apparent mobility (μ_{ap}) obtained at each position was plotted against the micrometer position (M), giving a parabolic profile. A quadratic equation was fitted by the least-squares method, and then differentiated and set to zero to solve for the maximum position, c.

The apparent mobility was then plotted against the dimensionless position (the Komagata plot), defined as $[(M - c)/h]^2$, where "h" is the actual center position, equivalent to half of the channel depth. The Komagata plot gives a straight line with equation:

$$\mu_{ap} = 1.86\mu_e \left(\frac{M - c}{h} \right)^2 + (\mu_e - 0.86\mu_{eo}). \qquad (16)$$

The true electrophoretic mobility (μ_e) and the contribution to the apparent mobility due to electroosmosis (μ_{eo}) can be determined from the slope and the intercept of the plot.

Using this technique, electrophoretic mobilities could be obtained for even smaller proteins, such as lysozyme.

Streaming Potential Measurements. Streaming potential measurements were made on both clean and protein-fouled membranes using the flat-plate streaming potential apparatus of Scales et al. (1992) and the through-pore streaming potential apparatus of Nyström et al. (1989, 1994). In the flat-plate apparatus, pure buffer or protein solutions were circulated through a capillary formed by two pieces of membrane, each resting on a Teflon slide on each side of the streaming potential cell and separated by a thin Teflon gasket to form a slit 0.012 cm in depth. The streaming potential developed across

Table 3. Summary of Experiments Conducted

Expt.	Protein	Buffer	pH	I (M)
No. 1	Hb	NaAc	4.6	0.040
No. 2	Hb	TRIS	8.2	0.040
No. 3	Lys	TRIS	8.1	0.040
No. 4	Hb	NaAc	4.6	0.075

a pair of platinized platinum electrodes, one located upstream of the flow and the other downstream, was measured as a function of the applied pressure gradient over the pH range 4 to 8. This limited pH range was chosen to cover the pH of the buffers used in the electrophoresis experiments [NaAc: useful pH range 4.0–5.4, pKa 4.75; TRIS: useful pH range 6.9–9.0, pKa 8.30; the electrophoresis experiments were carried out close to the pKa of the buffers to obtain the maximum buffering capacity (see Table 3)]. In the through-pore apparatus, buffer or protein solutions were forced through the membrane pores and the streaming potential developed was measured across a pair of Ag/AgCl electrodes located on both sides of the membrane. The maximum pH was restricted to 7.5 in this case to avoid damage to the electrodes under alkaline conditions.

The zeta potential and the streaming potential are related by the Helmholtz–Smoluchowski equation:

$$\zeta = \frac{\eta K}{D\epsilon_o}\frac{\Delta E}{\Delta P}, \tag{17}$$

where ζ is the apparent zeta potential, D is the dielectric constant of the medium, ϵ_o is the permittivity of vacuum, η and K are the viscosity and conductivity of the bulk solution, respectively, and $\Delta E/\Delta P$ is the streaming potential developed as a result of an applied pressure gradient. No corrections for the double-layer thickness (Rice and Whitehead, 1965) or surface conductance (Ghosh et al., 1953) were included.

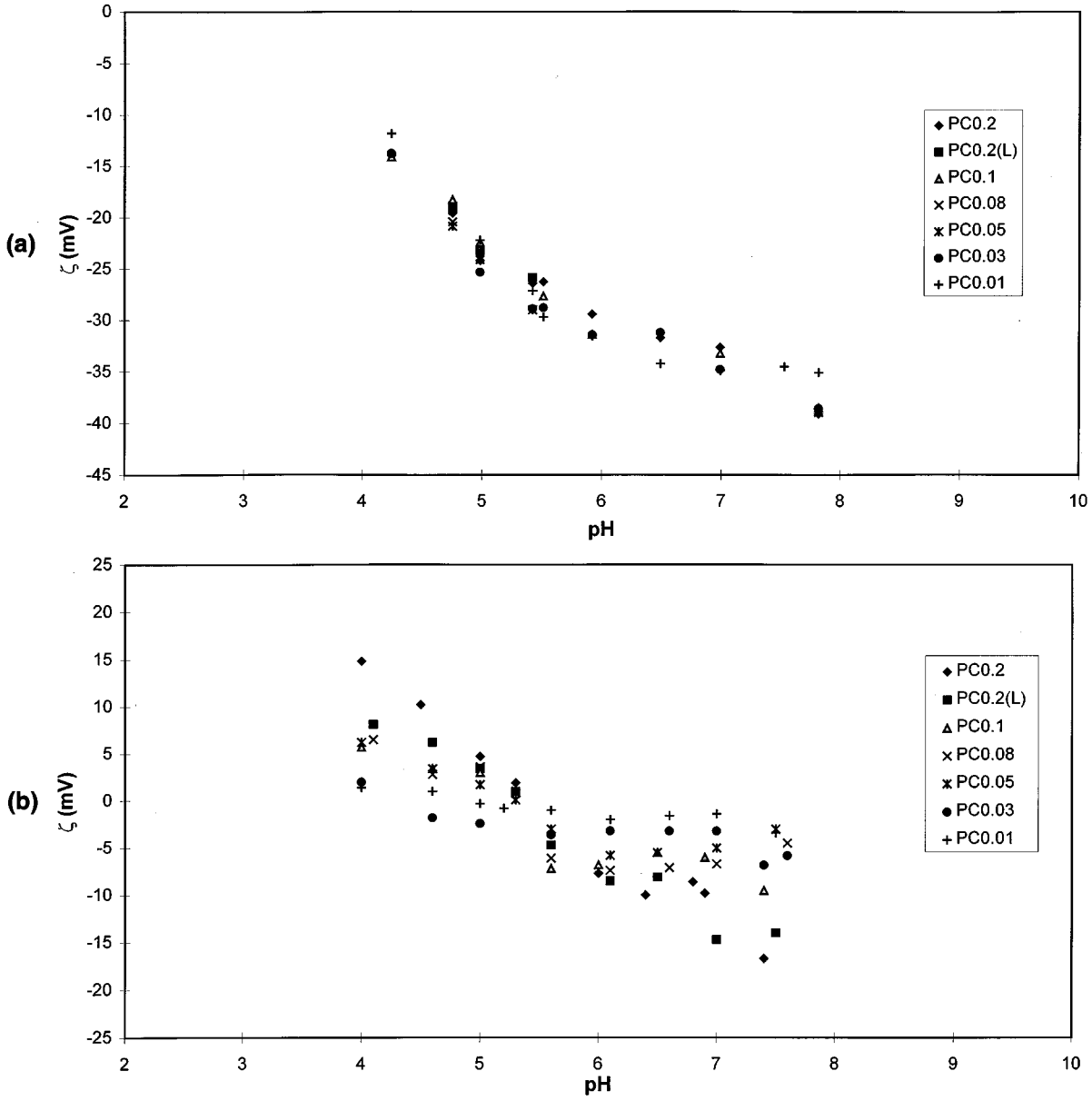

Figure 1. Apparent zeta potential vs. pH for clean membranes: (a) flat-plate technique; (b) through-pore technique.

It should be noted that the streaming potential measurements could not be made at the ionic strength used in the electrophoresis experiments, because this would give a high solution conductivity and consequently a small slope ($\Delta E/\Delta P$), which would reduce the accuracy of the measurements considerably. Hence the measurements were made at a lower ionic strength (10^{-3} M) at a range of pH values. In the experiments with protein-fouled membranes, a protein concentration of 0.1 mg/mL was used.

Membrane Pore-Size and Protein-Size Measurements. Additional measurements were made to obtain the protein and membrane pore sizes. Uncertainties in the protein size are noted for certain proteins that tend to self-associate. Measurements were done by photon correlation spectroscopy using the *Malvern-4700*. The membrane pore sizes were measured using field emission scanning electron microscopy (FESEM) on the *Philips XL-30 FEG* with the membrane specimens precoated with platinum in a magnetron sputter coater *Xenosput* from Dynavac Engineering. Although these membranes are often assumed to contain ''model pores'' ideal for studies in membrane transport, several workers have reported irregularities such as multiple pores, irregular shape, and the existence of a size distribution (Dietz et al., 1992; Kim and Stevens, 1997; Kim et al., 1994b; Martinez-Villa et al., 1988; Kim et al., 1992).

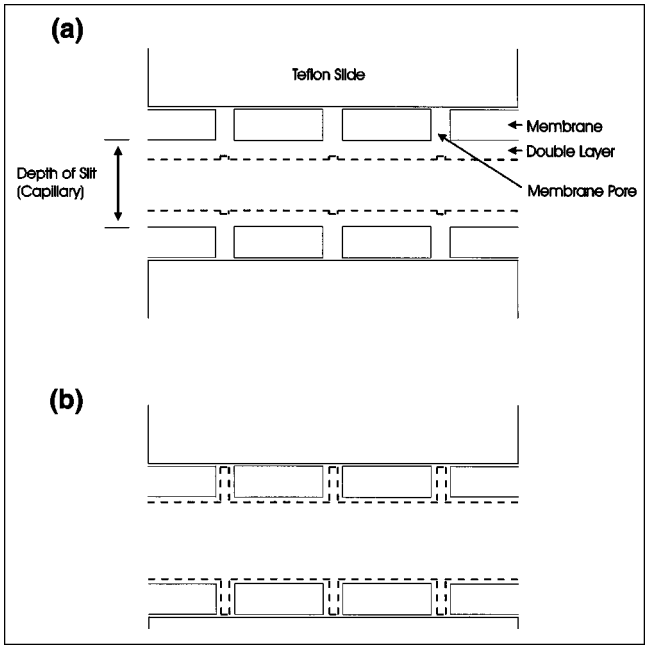

Figure 2. Electrical double layer in relation to the membrane pore size in the flat-plate streaming potential cell for: (a) thick; (b) thin double layers.

Results and Discussion

Comparison of streaming potential through membrane pores and over the membrane surface

Results for the apparent zeta potentials of clean membranes as illustrated in Figures 1a and 1b show substantial differences between the two measurement techniques. While the through-pore measurements show a pore-size dependence for the clean membranes, the measurements obtained using the flat plate technique were the same, within experimental error, for all membranes. This is not surprising, as the distance between the two pieces of membrane (the slit) was kept constant for all flat-plate measurements, and the streaming potential was measured over the membrane surface rather than through the pores. The membrane pore size is not expected to play an important role in these measurements, as the double-layer thickness is of comparable magnitude to the pore dimensions (double-layer thickness 9.6 nm at 10^{-3} M ionic strength; pore radii 5–100 nm according to the manufacturer's specifications). Figures 2a and 2b illustrate this for the two limiting cases, with thick and thin double layers, respectively. Overall, more scatter was noted with the through-pore measurements, possibly due to heterogeneous pore sizes and nonuniform pore-size distributions.

The experimental membrane isoelectric point obtained using the flat-plate technique is approximately 3.8 for all pore sizes, so that the zeta potential is negative throughout the entire pH range tested (pH 4 to 8). With the through-pore technique, the zeta potential changes from positive to negative as the pH increases. The isoelectric point ranges from 4.25 for the 0.01-μm membrane, to 5.4 for the 0.2-μm membrane. This increase in magnitude of the apparent zeta potential with increasing pore size was also observed by Kim et al. (1997) and has been explained by differences in the surface properties of the membrane pores. The different pore sizes are achieved by varying the degree of etching of the polycarbonate structure in strong alkaline solution after the thin plastic film is exposed to ionizing radiation and forms damaged tracks. The larger the pore size, the longer the etching period required, and hence a higher density of carboxyl groups is formed at the pore surface.

The observation of opposite charges on the membrane surface and along the pore walls for the two measurement techniques from pH 4 to 4.25 (PC0.01) or 5.4 (PC0.2) seems to suggest the presence of different functional groups even though the application of a wetting agent after the radiation and etching steps is expected to give uniform surface properties for the membrane as a whole. Similar trends (results not shown) were observed with both techniques when the buffer solutions were replaced by an indifferent electrolyte, KCl, at the same ionic strength.

Differences in zeta potential values or membrane isoelectric points under identical experimental conditions have also been reported by Kim et al. (1996) and Szymczyk et al. (1997, 1998) in their comparisons between the streaming potential and electroosmosis measurement techniques. Kim et al. (1996) explained the observations by a complicated theory of bulk ion redistribution due to the applied field causing a change in the conductivity, and the creation of concentration gradients that opposed ion transport toward the electrodes. On the other hand, Szymczyk et al. (1997, 1998) postulated that the shear planes, where the zeta potentials are defined, are not localized in the same position for the two different techniques.

The observations for the hemoglobin-fouled membranes (Figure 3) are quite different from those for the clean membranes. No pore size dependence was observed even with the

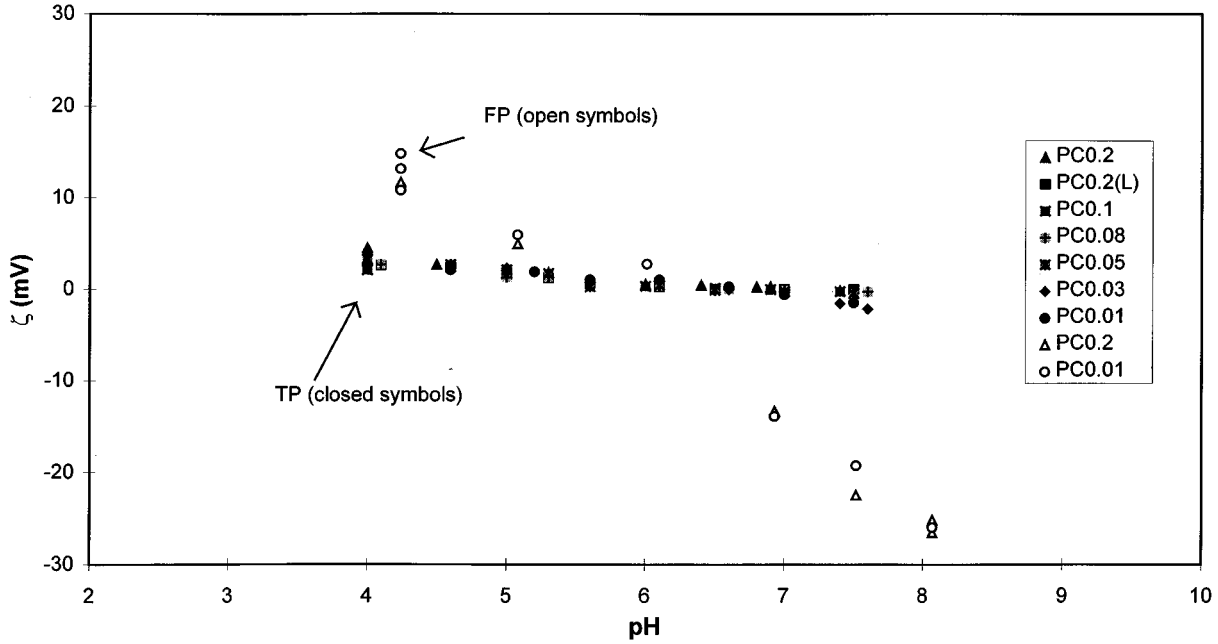

Figure 3. Apparent zeta potential vs. pH for Hb-fouled membranes (through-pore or flat-plate technique).

through-pore measurements due to complete modification of all pore sizes. Further, for both techniques, the isoelectric point of the fouled membranes became close to that of the foulant. Both of these observations are in agreement with Nyström (1994).

It should be noted that only *apparent* zeta potentials have been presented here when in fact the measurements were carried out in a range of electrokinetic radii for which corrections to the ideal Helmholtz–Smoluchowski equation may be required. Even when corrections for surface conductance and double-layer thickness were applied, the through-pore zeta potentials still did not merge into one curve, and in some cases the zeta potentials for the larger pore-size membranes became lower than the smaller pore-size ones. Apparent zeta potential values are often used since the corrections do not take into account all of the phenomena associated with these measurements, such as the presence of fixed charges on the capillaries or membrane pores (Oldham et al., 1963; Levine et al., 1975; Anderson and Koh, 1977), distributed conductance and differences in ionic mobilities of coions and counterions of fixed charge (Hildreth, 1970), and changes in dielectric constant or viscosity (Dukhin and Derjaguin, 1974; Grahame, 1950).

The Helmholtz–Smoluchowski equation is known to underestimate the zeta potential, and this partly explains why the through-pore zeta potentials are always lower in magnitude than the flat plate ones (corrections to the flat-plate zeta potentials are not important because of the wider flow channel than the membrane pores). In addition, while the flat-plate streaming potential experimental setup can be represented by a rectangular geometry (flow through a rectangular slit), the through-pore one is of a cylindrical geometry (flow through cylindrical pores). It is understood from the theory of electrostatics that the electric potential decays less rapidly with distance from a charged surface with the rectangular geometry (Overbeek and Bijsterbosch, 1979). Based on this it would seem more appropriate to use the through-pore zeta potentials in the transport of proteins through membrane pores, and the flat-plate zeta potentials in crossflow filtrations where the fluid flows tangentially to the membrane surface.

Membrane imaging using field-emission scanning electron microscopy

The electron micrographs in Figures 4a and 4b show the different morphologies of the two sides of the track-etched membranes of pore size 0.2 μm. The ''matte'' side shows more roughness and irregularities in pore size and shape than the ''shiny'' side. In some instances the pores penetrate at an angle to the membrane surface rather than perpendicular to it. Both sides also show an occurrence of multiples (overlapping of single pores). A smaller pore-size distribution and more regular pore shape is shown in Figure 4c for the lower pore-density membrane.

The average pore sizes obtained from the micrographs, considering only regular pores with no pore overlap, are given in Table 4. Also shown are plots of the dimensions of the measured pores (Figures 5a and 5b) where ''X-diameter'' and ''Y-diameter'' are the horizontal and vertical diameters, respectively. It should be noted that the definition of these diameters is somewhat arbitrary, as it depends on the orientation of the membrane specimens inside the microscope. Nevertheless, an ''ideal'' pore is classified as one that has the same pore size as given by the manufacturer, and one that has a circular cross section.

The existence of a pore-size distribution is illustrated in Figures 5a and 5b, for the membranes PC0.2 and PC0.05, respectively (all other membranes showed the same trends).

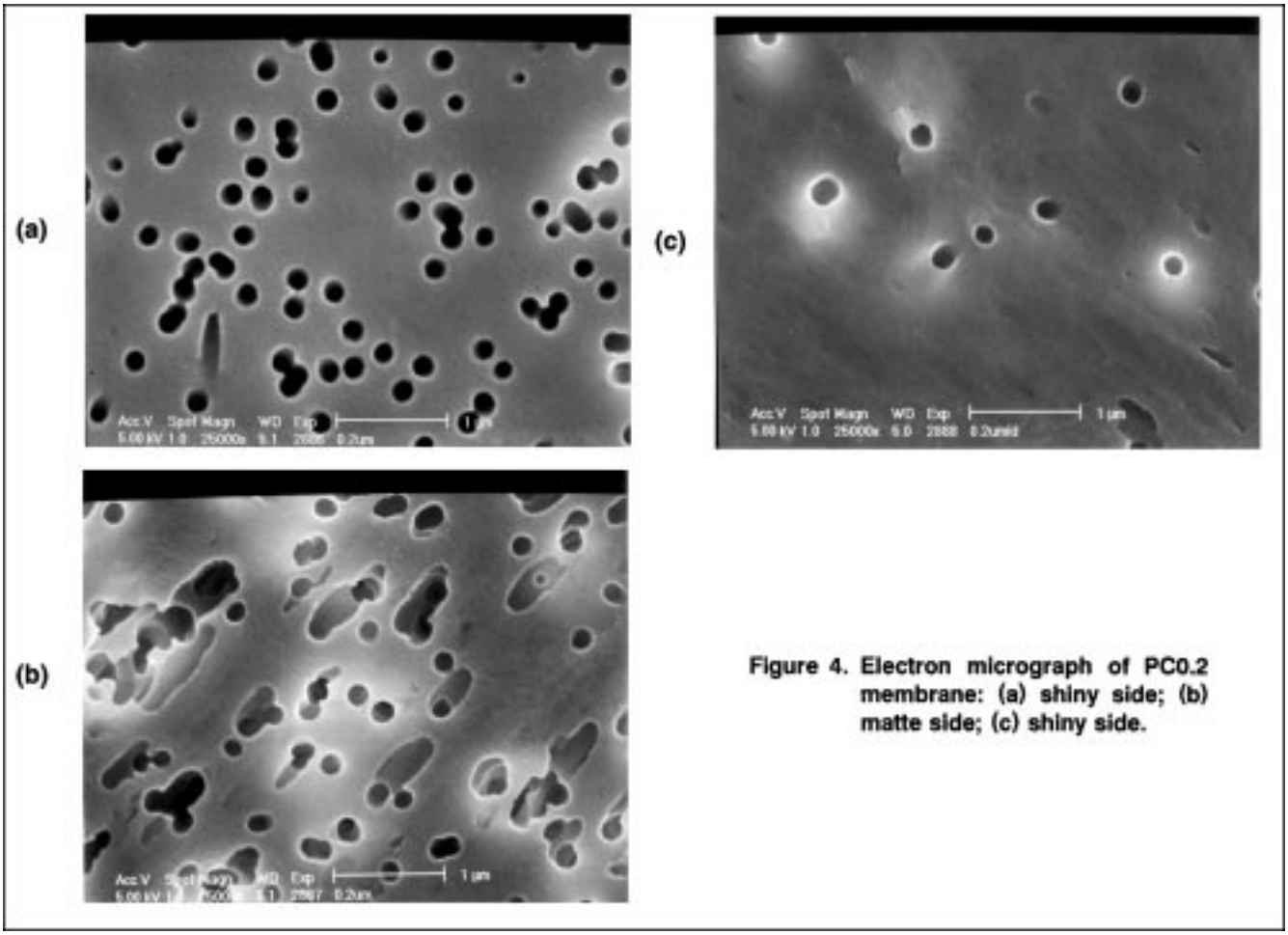

Figure 4. Electron micrograph of PC0.2 membrane: (a) shiny side; (b) matte side; (c) shiny side.

Also, many of the measured pore sizes do not fall onto the 45° line, indicating that the cross sections of the pores may be better described as elliptical rather than circular. From Table 4, it can be seen that while on average the measured pore sizes are in excellent agreement with the manufacturer's specifications for the larger pore sizes, this is not so for the smallest pore sizes. The underestimation of the measured pore sizes for the PC0.08 and PC0.05 membranes may be due to the metal coating (platinum thickness ~ 2 nm) required to increase the conductivity of the samples. On the other hand, the overestimation of the pore sizes for the PC0.01 membrane may be due to the inability to see the smaller pores. Although the resolution of the FESEM is 2 nm, this is true only of a high-conductivity, electron-dense sample (personal communication with J. L. Carpenter, electron microscopist, The University of Melbourne). More error in the measured pore sizes is also expected for the PC0.01 and PC0.03 membranes, as these were considerably more difficult to image.

Although some variation is expected between different batches of membrane samples, a general observation is that the membrane pore sizes obtained from atomic force microscopy are larger than those from the FESEM experiments (Table 4). In fact, measured values between 13 and 80% higher than the expected ones have been reported (Dietz et al., 1992). The atomic-force microscope can only probe the pores at the very top of the membrane surface, so the overestimation of the pore sizes may be an indication that the membrane pore entries are funnel-shaped with rounded corners, instead of having straight sides with sharp corners.

Table 4. Measured Pore Sizes of the Track-Etched Membranes

Membrane	Meas. Pore Dia. (μm)	Meas. Pore Dia. from Literature (μm)
PC0.2	0.202 ± 0.077	0.088 (Nyström, 1997)
PC0.2 (L)	0.184 ± 0.045	0.112 (Nyström, 1997)
PC0.1	0.097 ± 0.043	0.074 (Kim and Stevens, 1997) 0.1133* (Dietz et al., 1992)
PC0.08	0.066 ± 0.029	0.062 (Kim and Stevens, 1997)
PC0.05	0.044 ± 0.019	0.039 (Kim and Stevens, 1997) 0.065* (Dietz et al., 1992)
PC0.03	0.032 ± 0.017	0.021 (Kim and Stevens, 1997)
PC0.01	0.018 ± 0.010	0.014 (Kim and Stevens, 1997) 0.018* (Dietz et al., 1992)

*From AFM images (all others: from FESEM images).

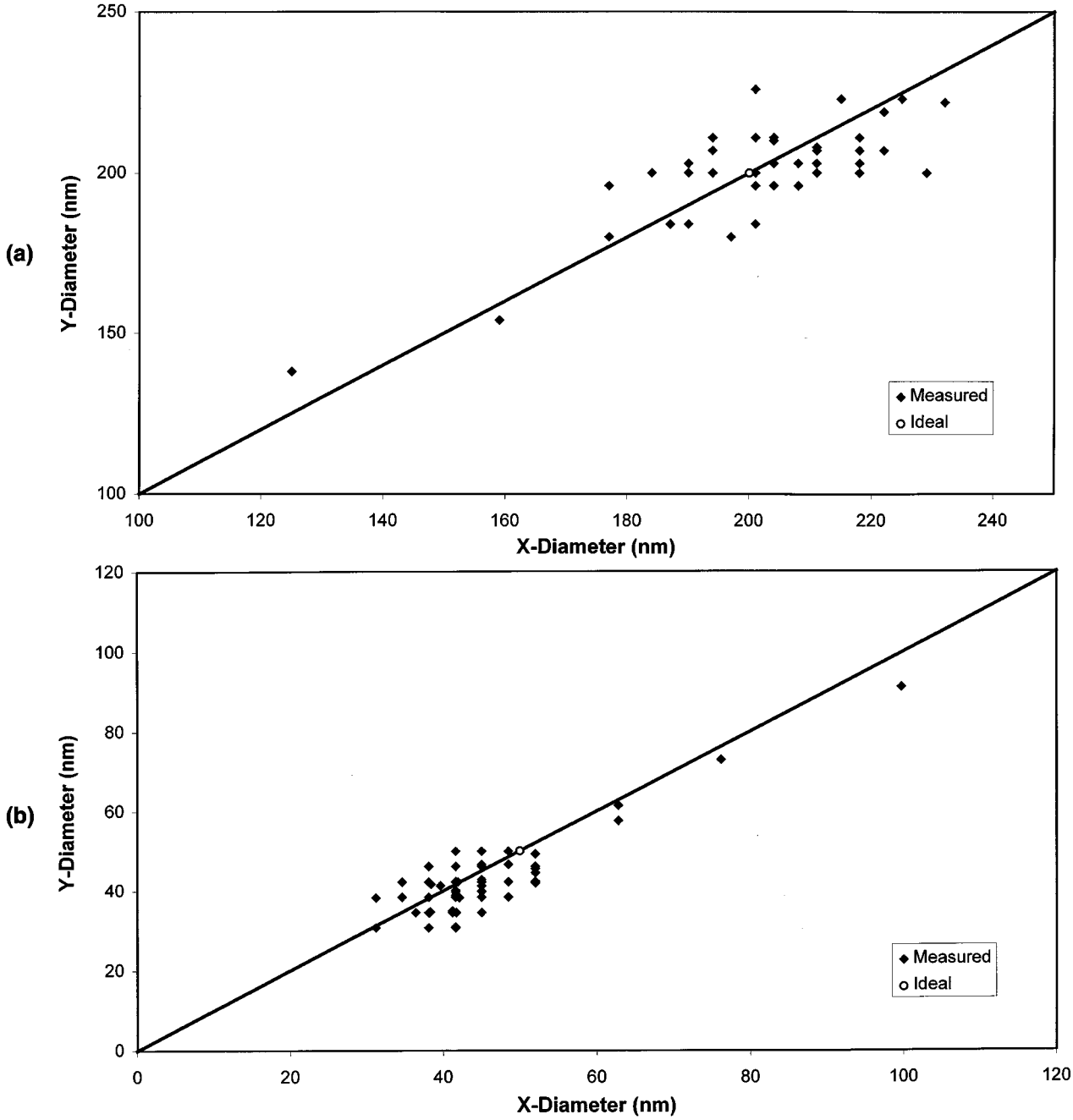

Figure 5. Measured pore sizes: (a) PC0.2; (b) PC0.05.

Comparison of electrophoretic mobilities

Comparison was made between the free-solution mobilities obtained using the *Coulter DELSA 440*, those obtained using the membrane-electrophoresis apparatus with the largest membrane pore size (0.2 μm), and those predicted using the Debye–Hückel–Henry (DHH) theory. The results, summarized in Table 5, show good agreement of the experimental results with theory. They also indicate that little hindrance to protein transfer occurs when the membrane pore size is large compared to the protein size and the thickness of the electrical double layers.

Dynamic light-scattering results

Results from the dynamic light-scattering measurements, given as volume-based equivalent spherical diameters (d_{vol}), together with their proportion (%) in solution, are shown in Table 6. The experiments were conducted after passage of the protein solutions through 0.1-μm filters to remove dust particles and other contaminants, and any large protein aggregates initially in solution.

Comparison with data of protein sizes in the literature (see Table 2) indicate definite agglomeration of hemoglobin in NaAc buffer and lysozyme in TRIS buffer, but not hemoglobin

Table 5. Comparison of Measured and Predicted Protein Mobilities

Expt.	μ_{DELSA} ($cm^2/V \cdot s$)	$\mu_{PC0.2}$ ($cm^2/V \cdot s$)	μ_{DHH} ($cm^2/V \cdot s$)
No. 1	1.29×10^{-4}	1.23×10^{-4}	1.17×10^{-4} ($a = 4.8$ nm*, $z^{**} = 22$)
No. 2	-1.10×10^{-4}	-1.08×10^{-4}	-1.28×10^{-4} ($a = 4.03$ nm†, $z = -18$)
No. 3	1.59×10^{-4}	1.56×10^{-4}	1.51×10^{-4} ($a = 1.9$ nm††, $z = 6.5$)
No. 4	1.01×10^{-4}	1.02×10^{-4}	0.94×10^{-4} ($a = 4.8$ nm‡, $z = 22$)

*Size of hemoglobin monomer in NaAc buffer (Zhang, 1996).
**z = protein charge. Obtained from titration curves (O'Connor, 1994; Zhang, 1996).
†Dynamic light-scattering results. See Table 6.
††Literature value for size of lysozyme monomer. See Table 2.
‡As for Expt. No. 1, Table 5.

in TRIS buffer. Fairly consistent results could be obtained for hemoglobin in TRIS buffer solution, so an average protein size is given. For hemoglobin in NaAc buffer and lysozyme in TRIS buffer, the observation of continually increasing protein sizes (Table 6) is evidence that agglomeration of these proteins under the given conditions is a dynamic process.

Membrane-electrophoresis of model proteins and the validation of the theory of Ennis et al.

A series of electrophoresis experiments was conducted through membranes of different pore sizes in order to examine their effect on protein mobilities. In each case the change in initial absorbance was less than 4%, indicating that protein adsorption, desorption, or any other type of irreversible fouling was negligible, at least under the experimental conditions tested. Despite the differences noted between the two sides of the membranes as shown previously, surprisingly little difference in the experimental mobilities was observed upon reversal of the membrane direction. The results were also reproducible within 90–95% using either the same piece of membrane, or a different piece of membrane within the same batch.

Graphs of relative mobility vs. size ratio for the four sets of experiments are given in Figures 6a to 6d. Zeta potentials for hemoglobin-fouled membranes were given previously (Figure 3), over a range of pH values. Zeta potentials for lysozyme-fouled membranes have also been measured, using the flat-plate technique at 10^{-3} M ionic strength and at the same pH as for the electrophoresis experiments. These (ζ_w), together with the protein zeta potentials (ζ_p) estimated from the experimental mobilities and the Debye–Hückel–Henry theory, are given in Table 7.

Strictly speaking only the through-pore membrane zeta potentials should be used, as the experimental setup mimics more closely the membrane-electrophoresis experiments. However, the use of these values is complicated by the necessity of corrections to take into account the double-layer thickness and other factors, and previously it was found that such corrections did not rectify the problem of underestimating the zeta potentials from the Helmholtz–Smoluchowski equation.

Due to these difficulties, the assumption of zero zeta potential ratio (γ) was made, and this can be justified as follows:

- The flat plate zeta potential ratios (Table 7), which did not require corrections to the ideal streaming/zeta potential equation, gave values close to zero in most cases. These measurements were carried out at a low ionic strength (10^{-3} M) because high conductivity solutions would greatly reduce the accuracy of the measurements [Zhang (1996) found that even an ionic strength of 10^{-2} M was enough to cause deviations from linearity in the slope $\Delta E/\Delta P$]. In the electrophoresis experiments, much higher ionic strengths were used (0.04 M). Lower zeta potentials are expected due to compression of the electrical double layers.

- The hydrophilic polycarbonate membranes used in the experiments are known to exhibit low protein binding capacities (PORETICS, 1996), thus giving a low zeta potential ratio. (In the discussion of the through-pore streaming potential results, it was previously explained that the zeta potential of the fouled membranes was close to the zeta potential of the protein due to complete modification of all pores, implying complete coverage of the pore surface by the protein. It should be noted that in the streaming potential measurements, the protein solution was forced through the membrane pores. The conditions were more gentle in the electrophoresis experiments and thus less conducive to protein adsorption.) This was confirmed by electron micrographs of protein-fouled membranes after electrophoresis, which showed remarkable similarities to the clean membranes, with

Table 6. Measured Protein Sizes

	Protein	Conditions	d_{vol} (nm)	%	Remarks
(i)	Hb	NaAc buffer $I = 0.04$ M pH = 4.6	39.2 401.7	98.8 1.2	
(ii)	Hb	NaAc buffer $I = 0.04$ M pH = 4.6	138.5 1,077.0 1,542.2	44.1 34.4 21.5	Repeat of experiment (i) after 2 days
(iii)	Hb	NaAc buffer $I = 0.04$ M pH = 4.6	46.4 360.3	72.2 27.8	
(iv)	Hb	NaAc buffer $I = 0.04$ M pH = 4.6	65.2 1,288.2	93.0 7.0	Repeat of experiment (iii) after 15 min
(v)	Hb	TRIS buffer $I = 0.04$ M pH = 8.2	8.1	100	Average of 3 experiments (results quite reproducible)
(vi)	Lys	TRIS buffer $I = 0.04$ M pH = 8.1	6.6	100	
(vi)	Lys	TRIS buffer $I = 0.04$ M pH = 8.1	570.0 11,767.4	74.7 25.3	Repeat of experiment (vi) after 2 days

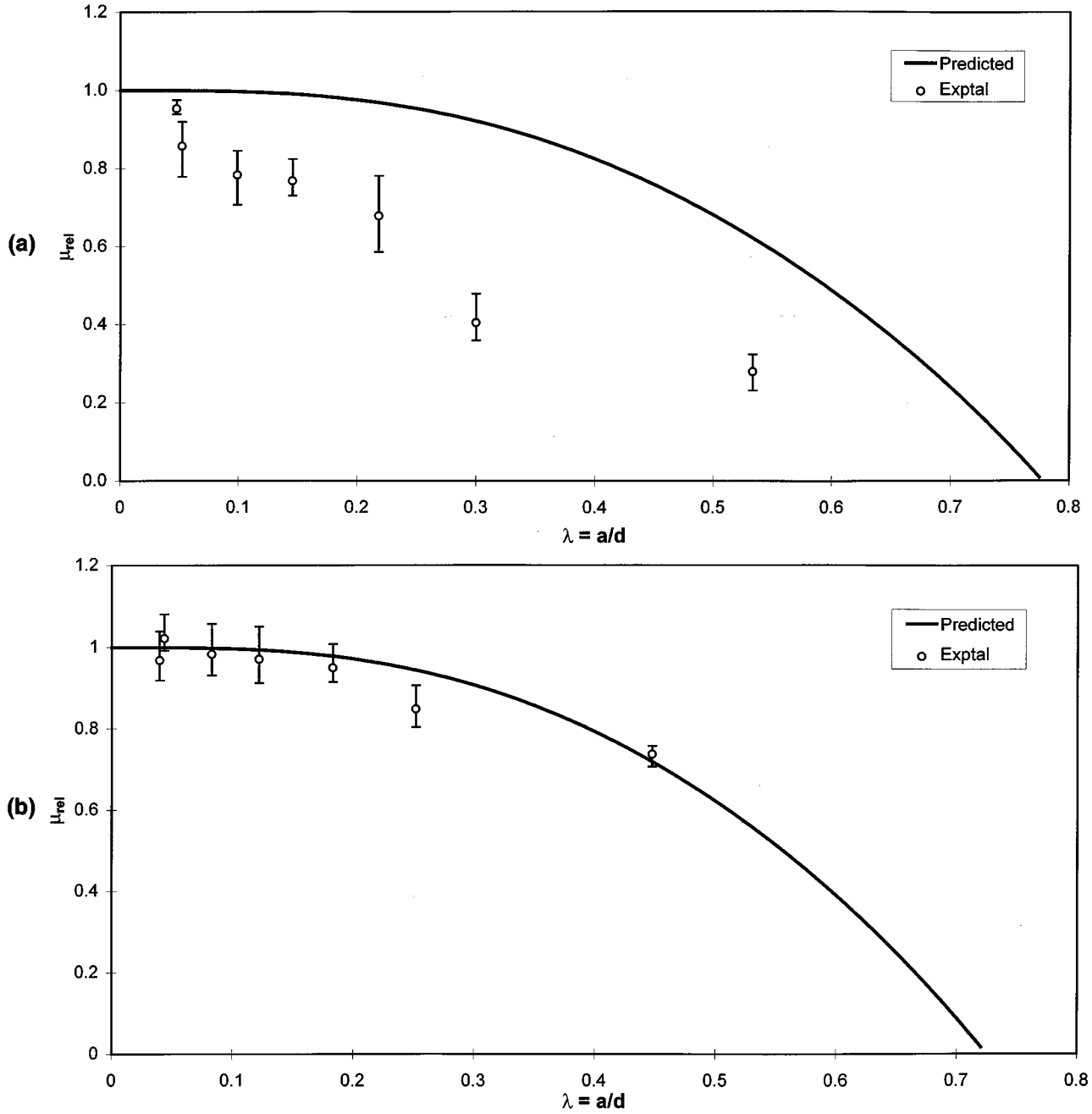

Figure 6. Relative mobility vs. size ratio: (a) Expt. No. 1, Hb in NaAc, I = 0.04 M, pH = 4.6, κa = 3.1462; (b) Expt. No. 2, Hb in TRIS, I = 0.04 M, pH = 8.2, κa = 2.6414 (*continued*).

little evidence of protein adsorption and no apparent reduction in the membrane pore size. For example, the average pore size for a clean PC0.2 membrane sample was 0.202 μm, and that for a fouled sample was 0.201 μm.

• Only positive zeta potential ratios are observable in practice. Thus, in the limit of negligible protein adsorption, a zeta potential ratio of zero seems to be a reasonable choice.

Comparison of the experimental results with the theoretical curves with $\gamma = 0$ indicate a more pronounced reduction in relative mobility for the cases where protein agglomeration was significant (Figures 6a, 6c, 6d), but excellent agreement with theory where the protein remained as a monomer (Figure 6b). For example, the relative mobility decreased from 1 to 0.28 for hemoglobin in NaAc buffer of ionic strength 0.04 M, but only to 0.74 for the same protein in TRIS buffer, as predicted by the theory. Increasing the NaAc buffer ionic strength to 0.075 M did not improve the model predictions, indicating that protein agglomeration was still significant.

A negative zeta potential ratio, which gives rise to a pronounced reduction in relative mobility, cannot explain the results in Figures 6a, 6c, and 6d, as the membrane after protein adsorption will take on the same charge sign as the protein

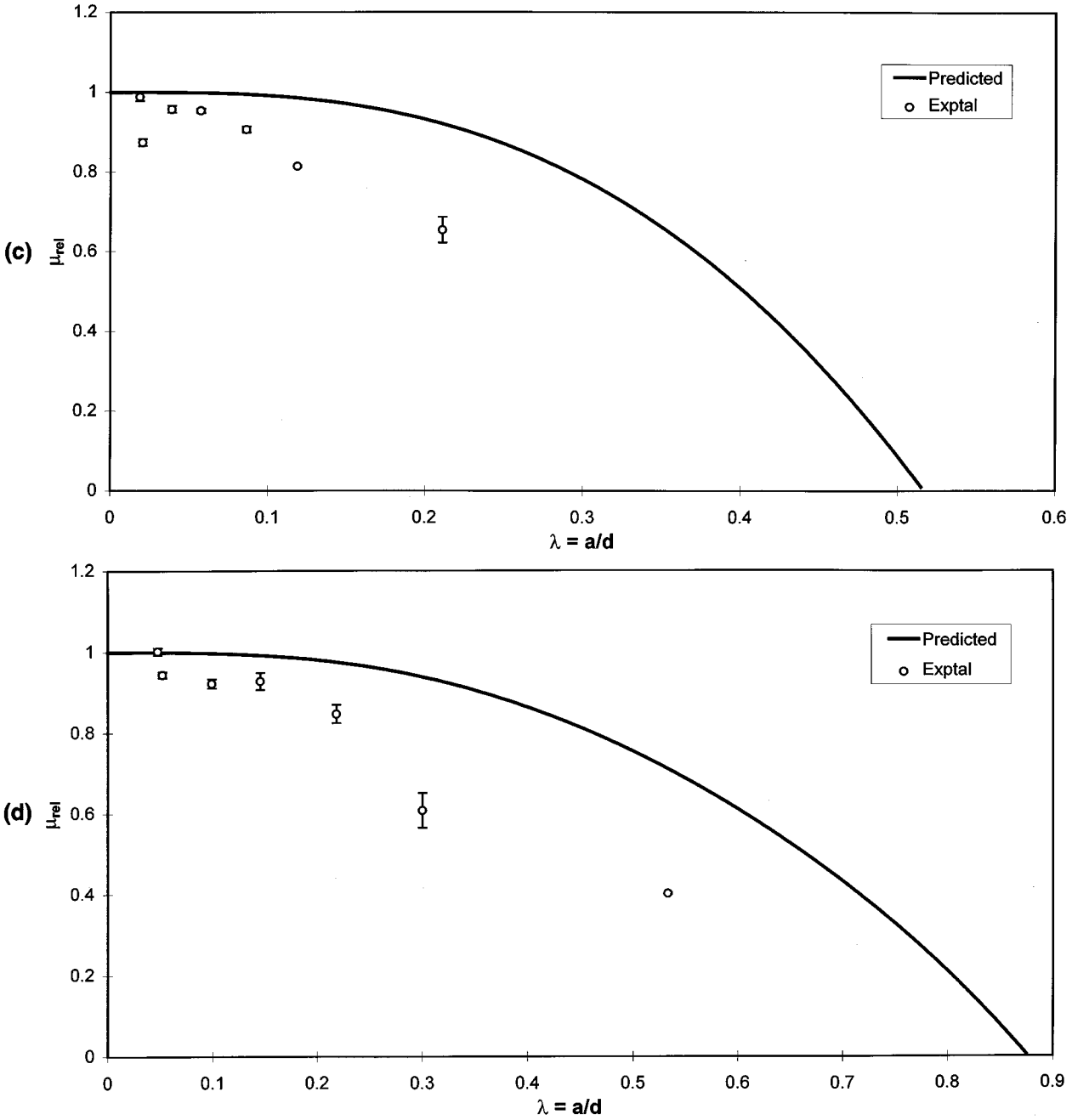

Figure 6. (*Continued*) Relative mobility vs. size ratio: (c) Expt. No. 3, Lys in TRIS, I = 0.04 M, pH = 8.1, $\kappa a = 1.2454$; (d) Expt. No. 4, Hb in NaAc, I = 0.075 M, pH = 4.6, $\kappa a = 4.3081$.

itself. Instead of displaying a higher mobility due to the higher charge-to-size ratio of the protein agglomerates, the observation of lower mobilities through the membrane pores can be attributed to the greater interaction between the larger particles with the membrane pore walls. It should be noted that these figures were plotted with the size of the protein *monomers* (Table 5), as no protein aggregates of the observed sizes (Table 6) should pass through the smaller pores. Nevertheless, no improvements were noted even when the graphs (not shown) were plotted with the size of the aggregates. This is probably due to the dynamic agglomeration process, giving rise to a strong variation in protein sizes with time, and consequently causing uncertainties in the fitting of experimental results to theory. No improvements were noted when the model was applied with the pore diameter reduced in size due to protein adsorption.

Table 7. Some Experimental Parameters for the Theoretical Model

Expt.	$\zeta_{w,TP}$ (mV)	$\zeta_{w,FP}$ (mV)	ζ_P (mV)	$\gamma_{TP} = \zeta_{w,TP}/\zeta_P$	$\gamma_{FP} = \zeta_{w,FP}/\zeta_P$
No. 1	2.47	8.4	19.8	0.13	0.42
No. 2	−2.00	−25.8	−18.0	0.11	1.42
No. 3	—	8.7	27.3	—	0.32
No. 4	2.47	8.4	16.6	0.15	0.51

Based on the criteria $\kappa(d-a)>6$ and $\kappa d>10$ for no double layer overlap, the theory of Ennis et al. (1996) is expected to be valid for a protein-pore-size ratio of less than around 0.5 (less for lower κa). Unfortunately the actual pore sizes of the membranes did not allow a wider range of size ratios to be obtained ($\lambda>0.5$) with the chosen proteins, and therefore it was not possible to ascertain in this work the actual limitations of the theory. It is clear, however, that the theory works well for λ, down to 0.5 for these conditions.

Conclusions

The electrochemical characteristics of both clean and protein-fouled polycarbonate track-etched membranes were examined using two independent techniques, one of which measures the streaming potential over the membrane surface and the other through the membrane pores. Some differences in the experimental results were observed. However, both techniques showed that the membranes after protein adsorption took on the same charge sign as the protein itself. Further, the low protein adsorption capacities of these membranes were confirmed by the low zeta potential of the fouled membranes.

The physical properties of the membranes, in particular their pore size and surface morphology, were also examined using field-emission scanning electron microscopy. Some discrepancies between the rated and measured pore size were noted, as were irregularites in the pore shape and structure.

The performance of the membrane-electrophoresis apparatus was tested and the presence of the membrane was found to be effective in controlling flow and mixing of solutions, while at the same time offering little hindrance to protein transfer if the correct membrane pore size was chosen.

Protein agglomeration was found to occur under certain solution conditions, causing greater interaction between the larger particles and the membrane pore walls, and consequently a lower effective mobility through membranes than expected. The theoretical model of Ennis et al. (1996), however, was shown to be adequate in describing the transport of protein monomers through different membrane pore sizes.

The theoretical model could only be tested over a limited range of the protein pore-size ratio. The use of more well-characterized colloid particles, such as a monodispersed solution of particles with well-defined particle size and surface charge characteristics, will better illustrate the limitations of the theory of Ennis et al. (1996).

The present work only deals with the electrophoresis of dilute single-protein solutions through membrane pores. The electrophoresis of proteins in concentrated multicomponent suspensions, or the separation of proteins from mixtures will further complicate the analyses. We plan to investigate these in our future studies.

Acknowledgments

The authors gratefully acknowledge support for this work from the Advanced Minerals Products Special Research Centre, the University of Melbourne Collaboration Grants Scheme, for J. M. Perera to visit the Lappeenranta University of Technology, Finland, to use the facilities for the streaming potential measurements, and an Australian Postgraduate Award for A. K. Ho. We also thank Dr. Peter Scales (School of Chemistry) and Jocelyn Carpenter (School of Botany) for valuable advice and helpful discussions on various aspects of this work.

Literature Cited

Anderson, J. L., and W.-H. Koh, "Electrokinetic Parameters for Capillaries of Different Geometries," *J. Colloid. Int. Sci.*, **59**, 149 (1977).

Bier, M., "Preparative Electrophoresis Without Supporting Media," *Electrophoresis: Theory, Methods and Applications*, M. Bier, ed., Vol. 1, Chapter 7, Academic Press, New York, p. 263 (1959).

Bier, M., N. B. Egen, T. T. Allgyer, G. E. Twitty, and R. A. Mosher, "New Developments in Isoelectric Focusing," *Peptides, Structure and Biological Function: Proc. Amer. Peptide Symp.*, E. Gross and J. Meienhofer, eds., Pierce Chemical Co., Rockford (1979).

Causserand, C., M. Nyström, and P. Aimar, "Study of Streaming Potentials of Clean and Fouled Ultrafiltration Membranes," *J. Memb. Sci.*, **88**, 211 (1994).

Cantor, C. R., and P. R. Schimmel, *Techniques for the Study of Biological Structure and Function, Biophysical Chemistry*, Part II, Freeman, San Francisco (1980).

Chae, K. S., and A. M. Lenhoff, "Computation of the Electrophoretic Mobility of Proteins," *Biophys. J.*, **68**, 1120 (1995).

Cogoli, A., and A. Tschopp, "Biotechnology in Space Laboratories," *Adv. Biochem. Eng.*, **22**, 1 (1982).

Coulter DELSA 440 Product Reference Manual, Langley Ford Instruments, Amherst (1988).

Dietz, P., P. K. Hansma, O. Inacker, H. D. Lehmann, and K. H. Hermann, "Surface Pore Structure of Micro- and Ultrafiltration Membranes Imaged with the Atomic Force Microscope," *J. Memb. Sci.*, **65**, 101 (1992).

Dukhin, S. S., and B. V. Derjaguin, "Electrokinetic Phenomena," *Surface and Colloid Science*, E. Matijevic, ed., Wiley, New York (1974).

Ehsani, N., *A Study on Fractionation and Ultrafiltration of Proteins with Characterised Modified and Unmodified Membranes*, Lappeenranta Univ. of Technology, Lappeenranta, Finland (1996).

Ehsani, N., S. Parkkinen, and M. Nyström, "Fractionation of Natural and Model Egg-White Protein Solutions with Modified and Unmodified Polysulfone UF Membranes," *J. Memb. Sci.*, **123**, 105 (1997).

Ennis, J., and J. L. Anderson, "Boundary Effects on Electrophoretic Motion of Spherical Particles for Thick Double Layers and Low Zeta Potential," *J. Colloid. Int. Sci.*, **185**, 497 (1997).

Ennis, J., H. Zhang, G. Stevens, J. Perera, P. Scales, and S. Carnie, "Mobility of Protein Through a Porous Membrane," *J. Memb. Sci.*, **119**, 47 (1996).

Fane, A. G., C. J. D. Fell, and A. Suki, "The Effect of pH and Ionic Environment on the Ultrafiltration of Protein Solutions with Retentive Membranes," *J. Memb. Sci.*, **16**, 195 (1983a).

Fane, A. G., C. J. D. Fell, and A. G. Waters, "Ultrafiltration of Protein Solutions Through Partially Permeable Membranes," *J. Memb. Sci.*, **16**, 211 (1983b).

Fox, S. W., and J. F. Foster, *Introduction to Protein Chemistry*, Wiley, New York (1957).

Ghosh, R., and Z. F. Cui, "Fractionation of BSA and Lysozyme Using Ultrafiltration: Effect of pH and Membrane Pretreatment," *J. Memb. Sci.*, **139**, 17 (1998).

Ghosh, B. N., S. C. Rakshit, and D. K. Chattoraj, "The Evaluation of True Zeta Potentials of Quartz Particles of Different Size from Measurements of Streaming Potential," *J. Indian Chem. Soc.*, **30**, 601 (1953).

Gobie, W. A., J. B. Beckwith, and C. F. Ivory, "High Resolution Continuous-Flow Electrophoresis," *Biotechnol. Prog.*, **1**, 60 (1985).

Gobie, W. A., and C. F. Ivory, "Recycle Continuous-Flow Electrophoresis: Zero Diffusion Theory," *AIChE J.*, **34**, 474 (1988).

Grahame, D. C., "Effects of Dielectric Saturation upon the Diffuse Double Layer and the Free Energy of Hydration of Ions," *J. Chem. Phys.*, **18**, 903 (1950).

Hanemaaijer, J. H., T. Robbertson, Th. van den Boomgaard, and J. W. Gunnick, "Fouling of Ultrafiltration Membranes: The Role of Protein Adsorption and Salt Precipitation," *J. Memb. Sci.*, **40**, 199 (1989).

Hannig, K., ''Preparative Electrophoresis,'' *Electrophoresis: Theory, Methods and Applications*, M. Bier, ed., Vol. II, Academic Press, New York (1967).
Heath, C. A., and G. Belfort, ''Synthetic Membranes in Biotechnology: Realities and Possibilities,'' *Bioseparation*, G. T. Tsao, ed., Springer-Verlag, Berlin (1992).
Higuichi, A., Y. Ishida, and T. Nakagawa, ''Surface Modified Polysulfone Membranes: Separation of Mixed Proteins and Optical Resolution of Tryptophan,'' *Desalination*, **90**, 127 (1993).
Hildreth, D., ''Electrokinetic Flow in Fire Capillary Channels,'' *J. Phys. Chem.*, **74**, 2006 (1970).
Hong, J., and C. K. Lee, ''Membrane Separation Coupled with Electrophoresis,'' *Ann. N. Y. Acad. Sci.*, **469**, 131 (1986).
Howell, J. A., V. Sanchez, and R. W. Field, eds., *Membranes in Bioprocessing—Theory and Applications*, Chapman & Hall, London (1993).
Hunter, J. B., ''In Focus and On the Move: Prospects for Electrophoresis in the Food Industry,'' *Bioseparation Processes in Foods*, R. K. Singh and S. H. H. Rizvi, eds., Dekker, New York (1995).
Hunter, R. J., *Zeta Potential in Colloid Science: Principles and Application*, Academic Press, London, p. 135 (1981).
Iritani, E., K. Ohashi, and T. Murase, ''Analysis of Filtration Mechanism of Dead-End Electro-Ultrafiltration for Proteinaceous Solutions,'' *J. Chem. Eng. Jpn.*, **25**, 383 (1992).
Keh, H. J., and J. L. Anderson, ''Boundary Effects on Electrophoretic Motion of Colloidal Spheres,'' *J. Fluid Mech.*, **153**, 417 (1985).
Keh, H. J., and S. B. Chen, ''Electrophoresis of a Colloidal Sphere Parallel to a Dielectric Plane,'' *J. Fluid Mech.*, **194**, 377 (1988).
Kim, K. J., V. Chen, and A. G. Fane, ''Characterizatioin of Clean and Fouled Membranes Using Metal Colloids,'' *J. Memb. Sci.*, **88**, 93 (1994a).
Kim, K. J., M. R. Dickson, V. Chen, and A. G. Fane, ''Applications of Field Emission Scanning Electron Microscopy to Polymer Membrane Research,'' *Micron Microsc. Acta*, **23**, 259 (1992).
Kim, K. J., A. G. Fane, M. Nyström, and A. Pihlajamäki, ''Chemical and Electrical Characterization of Virgin and Protein-Fouled Polycarbonate Track-Etched Membrane by FTIR and Streaming Potential Measurements,'' *J. Memb. Sci.*, **134**, 199 (1997).
Kim, K. J., A. G. Fane, M. Nyström, A. Pihlajamäki, W. R. Bowen, and H. Mukhtar, ''Evaluation of Electroosmosis and Streaming Potential for Measurement of Electric Charges of Polymeric Membranes,'' *J. Memb. Sci.*, **116**, 149 (1996).
Kim, K. J., and P. V. Stevens, ''Hydraulic and Surface Characteristics of Membranes with Parallel Cylindrical Pores,'' *J. Memb. Sci.*, **123**, 303 (1997).
Kim, K. J., P. V. Stevens, and A. G. Fane, ''Porosity Dependence of Pore Entry Shape in Track-Etched Membranes by Image Analysis,'' *J. Memb. Sci.*, **93**, 79 (1994b).
Le Bolay, N., and A. Ricard, ''Streaming Potential in Membrane Processes: Microfiltration of Egg Proteins,'' *J. Colloid. Int. Sci.*, **170**, 154 (1995).
Lehninger, A. L., *Principles of Biochemistry*, Worth, New York (1982).
Levine, S., J. R. Marriot, G. Neale, and N. Epstein, ''Theory of Electrokinetic Flow in Fine Cylindrical Capillaries at High Zeta Potentials,'' *J. Colloid. Int. Sci.*, **52**, 136 (1975).
Liu, Z., Z. Huang, J. Chong, H. Yang, F. Ding, and N. Yuan, ''Continuous Separation of Proteins by Multichannel Flow Electrophoresis,'' *Sep. Sci. Technol.*, **31**, 1427 (1996a).
Liu, Z., J. Wang, Z. Huang, F. Ding, Z. Shen, and N. Yuan, ''Continuous Separation of Proteins by Poly(vinyl Alcohol) Shielded Multichannel Flow Electrophoresis,'' *Biotechnol. Tech.*, **10**, 253 (1996b).
Lucas, D., M. Rabiller-Baudry, F. Michel, and B. Chaufer, ''Role of the Physicochemical Environment on Ultrafiltration of Lysozyme with Modified Inorganic Membrane,'' *Colloids Surf. A: Physicochem. Eng. Aspects*, **138**, 109 (1998).
Martinez-Villa, F., J. I. Arribas, and F. Tejerina, ''Quantitative Microscopic Study of Surface Characteristics of Track-Etched Membranes,'' *J. Memb. Sci.*, **36**, 19 (1988).
Metsämuuronen, S., M. Kulovaara, and M. Nyström, ''Characteristics Influencing Protein Fractionation by Ultrafiltration, Characterization of Interaction of Proteins with Membranes,'' ESMST Workshop, Lappeenranta, Finland (1997).
Miyama, H., H. Yoshida, and Y. Nosaka, ''Negatively Charged Polyacrylonitrile Graft Copolymer Membrane for Permeation and Separation of Plasma Proteins,'' *Makromol. Chem., Rapid Commun.*, **9**, 57 (1988).
Morrison, F. A., and J. J. Stuckel, ''Electrophoresis of an Insulating Sphere Normal to a Conducting Plane,'' *J. Colloid. Int. Sci.*, **33**, 88 (1970).
Musale, D. A., and S. S. Kulkarni, ''Relative Rates of Protein Transmission through Poly(acrylonitrile)-Based Ultrafiltration Membranes,'' *J. Memb. Sci.*, **136**, 13 (1997).
Nabe, A., E. Staude, and G. Belfort, ''Surface Modification of Polysulfone Ultrafiltration Membranes and Fouling by BSA Solutions,'' *J. Memb. Sci.*, **133**, 57 (1997).
Nakao, S., H. Osada, H. Kurata, T. Suru, and S. Kimura, ''Separation of Proteins by Charged Ultrafiltration Membranes,'' *Desalination*, **70**, 191 (1988).
Nyström, M., ''Streaming Potential Measurements, Characterization of Interactions of Proteins with Membranes,'' ESMST Workshop, Lappeenranta, Finland (1997).
Nyström, M., P. Aimar, S. Luque, M. Kulovaara, and S. Metsämuuronen, ''Fractionation of Model Proteins Using Their Physicochemical Properties,'' *Colloids Surf. A: Physicochem. Eng. Aspects*, **138**, 185 (1998).
Nyström, M., M. Lindström, and E. Matthiason, ''Streaming Potential as a Tool in the Characterization of Ultrafiltration Membranes,'' *Colloids Surf.*, **36**, 297 (1989).
Nyström, M., A. Pihlajamäki, and E. Ehsani, ''Characterization of Ultrafiltration Membranes by Simultaneous Streaming Potential and Flux Measurements,'' *J. Memb. Sci.*, **87**, 245 (1994).
O'Connor, A. J., ''Protein Electrophoresis through Porous Membranes,'' PhD Thesis, Dept. of Chemical Engineering, Univ. of Melbourne, Melbourne, Australia (1994).
O'Connor, A. J., H. R. C. Pratt, and G. W. Stevens, ''Electrophoretic Mobilities of Proteins and Protein Mixtures in Porous Membranes,'' *Chem. Eng. Sci.*, **51**, 3459 (1996).
Ohya, H., M. Kuromoto, N. Watanabe, K. Matsumoto, and Y. Negishi, ''Studies of Electrophoresis of Charged Organic Substances through Charged and Non-Charged Porous Membranes,'' *Membrane*, **14**, 329 (1989).
Oldham, I. B., F. J. Young, and J. F. Osterle, ''Streaming Potential in Small Capillaries,'' *J. Colloid. Int. Sci.*, **18**, 328 (1963).
Overbeek, J. Th. G., and B. H. Bijsterbosch, ''The Electrical Double Layer and the Theory of Electrophoresis,'' *Electrokinetic Separation Methods*, P. G. Righetti, C. J. van Oss, and J. W. Vanderhoff, eds., Elsevier/North-Holland, Amsterdam (1979).
Pelton, R., P. Miller, W. McPhee, and S. Rajaram, ''Strategies for Improving Electrophoresis Data from the Coulter DELSA,'' *Colloids Surf. A: Physicochem. Eng. Aspects*, **80**, 181 (1993).
Pihlajamäki, A., M. Nyström, S. Lentsch, and P. Aimar, *Separation of Proteins with Different Isoelectric Points in Aqueous Solution by Membrane Electrofiltration*, Lappeenranta Univ. of Technology, Lappeenranta, Finland (1993).
Pontié, M., X. Chasseray, D. Lemordant, and J. M. Lainé, ''The Streaming Potential Method for the Characterization of Ultrafiltration Organic Membranes and the Control of Cleaning Treatments,'' *J. Memb. Sci.*, **129**, 125 (1997).
PORETICS® — Microfiltration and Laboratory Products Catalogue, Poretics Corporation, Livermore, CA (1996).
Rice, C. L., and R. Whitehead, ''Electrokinetic Flow in a Narrow Cylindrical Capillary,'' *J. Phys. Chem.*, **69**, 4017 (1965).
Righetti, P. G., B. Barzachi, M. Luzzana, G. Manfredi, and M. Faupel, ''A Horizontal Apparatus for Isoelectric Protein Purification in a Segmented Immobilized pH Gradient,'' *J. Biochem. Biophys. Methods*, **15**, 189 (1987).
Scales, P. J., F. Grieser, T. W. Healy, L. R. White, and D. Y. C. Chan, ''Electrokinetics of the Silica-Solution Interface: A Flat Plate Streaming Potential Study,'' *Langmuir*, **8**, 965 (1992).
Saksena, S., and A. L. Zydney, ''Effect of Solution pH and Ionic Strength on the Separation of Albumin from Immunoglobulins (IgG) by Selective Filtration,'' *Biotechnol. Bioeng.*, **43**, 960 (1994).
Stamberger, P., ''The Method of Purifying and Concentrating Colloidal Dispersions by Electrodecantation,'' *J. Colloid. Sci.*, **1**, 93 (1946).
Szymczyk, A., A. Pierre, J. C. Reggiani, and J. Pagetti, ''Characteri-

zation of the Electrokinetic Properties of Plane Inorganic Membranes Using Streaming Potential Measurements,'' *J. Memb. Sci*., **134**, 59 (1997).

Szymczyk, A., P. Fievet, M. Mullet, J. C. Reggiani, and J. Pagetti, ''Comparison of Two Electrokinetic Methods—Electroosmosis and Streaming Potential—to Determine the Zeta Potential of Plane Ceramic Membranes,'' *J. Memb. Sci*., **143**, 189 (1998).

The Merck Index— An Encyclopedia of Chemicals, Drugs and Biologicals, 10th ed., M. Windholz, ed., S. Budavaii, co-editor, R. F. Blumetti, associate editor, and E. S. Ottenbein, assistant editor, Merck, Rahway, NJ (1983).

Tracey, E. M., and R. H. Davis, ''Protein Fouling of Track-Etched Polycarbonate Microfiltration Membranes,'' *J. Colloid. Int. Sci*., **167**, 104 (1994).

Van Eijndhoven, R. H. C. M., S. Saksena, and A. L. Zydney, ''Protein Fractionation Using Electrostatic Interactions in Membrane Filtration,'' *Biotechnol. Bioeng*., **48**, 406 (1995).

Walters, R. R., J. F. Graham, R. M. Moore, and D. J. Anderson, ''Protein Diffusion Coefficient Measurements by Laminar Flow Analysis: Methods and Application,'' *Anal. Biochem*., **140**, 190 (1984).

Weatherley, L. R., ''Electrokinetic Separation Processes for Biochemical Products,'' *Engineering Processes for Bioseparations*, L. R. Weatherley, ed., Butterworth-Heinemann, London (1994).

Zhang, H., ''Protein Electrophoresis Through Membranes,'' Masters Thesis, Dept. of Chemical Engineering, Univ. of Melbourne, Melbourne, Australia (1996).

Manuscript received Nov. 3, 1998, and revision received Apr. 1, 1999.